

# Structure of the nanocrystalline $\text{Fe}_{41}\text{Ni}_{20}\text{Co}_{20}\text{Zr}_7\text{B}_{12}$ alloy formed by ball milling

A. Grabias<sup>a,\*</sup>, D. Oleszak<sup>b</sup>, J. Kalinowska<sup>a</sup>, M. Kopcewicz<sup>a</sup>, J. Latuch<sup>b</sup>, M. Pękała<sup>c</sup>

<sup>a</sup> Institute of Electronic Materials Technology, Wólczyńska Street 133, 01-919 Warsaw, Poland

<sup>b</sup> Department of Materials Science and Engineering, Warsaw University of Technology, Wołoska 141, 02-507 Warsaw, Poland

<sup>c</sup> Department of Chemistry, University of Warsaw, Al. Zwirki i Wigury 101, 02-089 Warsaw, Poland

Available online 9 October 2006

## Abstract

High-energy ball milling technique with subsequent heat treatment were used to prepare the nanocrystalline  $\text{Fe}_{41}\text{Ni}_{20}\text{Co}_{20}\text{Zr}_7\text{B}_{12}$  alloy. The powder samples were obtained by mechanical milling of the melt-spun amorphous ribbon and by mechanical alloying of the mixture of pure elemental powders with the corresponding composition. Combined X-ray diffraction and Mössbauer spectroscopy measurements allowed the structural characterization of the samples. The powder prepared from the ribbon remained amorphous after milling for 27 h, while the milling of the mixture of crystalline elements for 200 h led to the formation of the nanocrystalline iron-based random solid solution. Differential scanning calorimetry results revealed three exothermic peaks, however, crystallization temperatures determined for the nanocrystalline powder were much lower than those obtained for the amorphous one. The first two stages correspond to the formation of the bcc FeCo nanograins. Annealing at higher temperatures caused the crystallization of the bcc phase followed by the formation of the iron-based borides. The magnetization measurements performed as a function of temperature confirmed the amorphous and crystalline states of the ball milled ribbon and mechanically alloyed elemental powders, respectively. The Curie temperature of the amorphous ribbon is markedly higher than that of the amorphous powder.

© 2006 Elsevier B.V. All rights reserved.

**Keywords:** Nanostructured materials; Mechanical alloying; X-ray diffraction; Mössbauer spectroscopy; Magnetic measurements

## 1. Introduction

It has been shown recently that soft magnetic nanocrystalline FeNiZrB alloys, prepared by the controlled crystallization from the amorphous precursors, exhibit low coercivity combined with improved mechanical properties [1]. In this work, we studied the nanocrystalline FeNiZrB alloy with addition of cobalt in order to increase the saturation magnetization. High-energy ball milling technique with subsequent heat treatment were used to form the nanocrystalline alloy. The ball milling has been used before to obtain amorphous and nanocrystalline FeNiCoZrB alloys [2–4].

In the present study, the  $\text{Fe}_{41}\text{Ni}_{20}\text{Co}_{20}\text{Zr}_7\text{B}_{12}$  alloy was first prepared as an amorphous ribbon by the melt-spinning. The powder samples were obtained in two ways: (i) by mechanical milling of the melt-spun ribbon and (ii) by mechanical alloying of the mixture of pure elemental powders with the corresponding composition. Structural characterization of the samples was

performed by X-ray diffraction and Mössbauer spectroscopy techniques. Differential scanning calorimetry measurements allowed us to study the crystallization behaviour of the amorphous and nanocrystalline powders. The dependence between the structure and magnetic properties of the ribbon and powder samples was studied by magnetization measurements at elevated temperatures.

## 2. Experimental details

The  $\text{Fe}_{41}\text{Ni}_{20}\text{Co}_{20}\text{Zr}_7\text{B}_{12}$  amorphous alloy was prepared in a ribbon form by the melt-spinning technique. The ribbon was 3 mm wide and about 40  $\mu\text{m}$  thick. About 5 g of the amorphous ribbon (cut into pieces) was subjected to high-energy ball milling for 27 h under an argon atmosphere. The Fritsch P5 planetary ball mill with steel vial and balls and 250 rpm was used. This mill was also used to prepare the  $\text{Fe}_{41}\text{Ni}_{20}\text{Co}_{20}\text{Zr}_7\text{B}_{12}$  alloy by high-energy ball milling of 10 g of the mixture of pure elemental powders for 200 h. Particle sizes of the obtained powders were below 10  $\mu\text{m}$ . In order to study the thermal behaviour of the as-milled powders the differential scanning calorimetry (DSC) analysis was performed with the scanning rate of 20  $\text{K min}^{-1}$ . The samples were nanocrystallized by heating in the calorimeter up to the characteristic crystallization temperatures determined from the DSC curves. Structural properties of the ribbon and powder samples were investigated by X-ray diffraction (XRD) and

\* Corresponding author. Tel.: +48 22 8353041; fax: +48 22 8645496.  
E-mail address: agrabias@itme.edu.pl (A. Grabias).

transmission Mössbauer spectroscopy. A standard powder diffractometer with Cu K $\alpha$  radiation was employed. The average grain size of the crystalline phases was estimated by Sherrer formula. All Mössbauer spectra were measured at room temperature using a  $^{57}\text{Co}$ -in-Rh source. The relative content of the phases present in the nanocrystalline samples was calculated as a ratio of the area of the relevant subspectrum to the total spectral area. Faraday balance was used for magnetization measurements at wide temperature range in the magnetic field up to 1.5 T.

### 3. Results and discussion

The powder prepared by ball milling of the as-quenched  $\text{Fe}_{41}\text{Ni}_{20}\text{Co}_{20}\text{Zr}_7\text{B}_{12}$  amorphous ribbon remained amorphous after milling for 27 h as revealed by Mössbauer spectroscopy (Fig. 1) and X-ray diffraction (Fig. 2) measurements. The Mössbauer spectrum of the as-milled powder (Fig. 1b) is typical for an amorphous, ferromagnetic alloy and resembles the spectrum of the starting as-quenched ribbon (Fig. 1a). Both spectra consist of six broad and overlapping lines indicating the distribution of the hyperfine fields, directly related to the diversity of local atomic arrangements around Fe atoms characteristic for amorphous alloys. The average val-

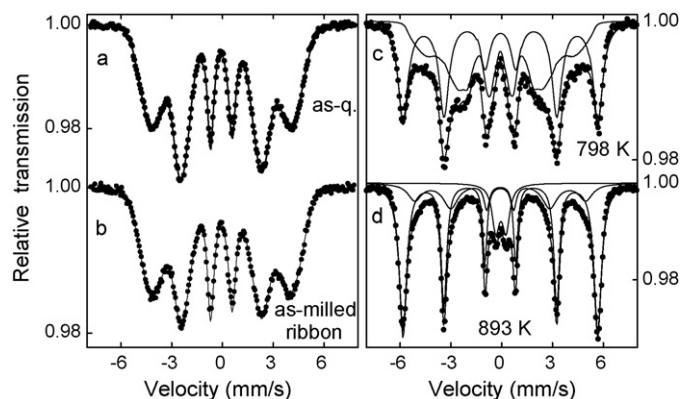


Fig. 1. Mössbauer spectra of the samples prepared from the ribbon: (a) in the as-quenched state, (b) after milling for 27 h, and (c and d) after heat treatment of the as-milled powders.

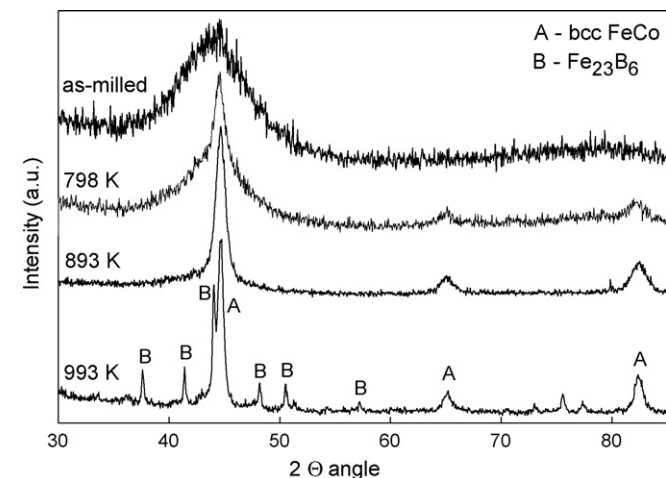


Fig. 2. XRD patterns of the as-milled and heated powders prepared by ball milling of the ribbon.

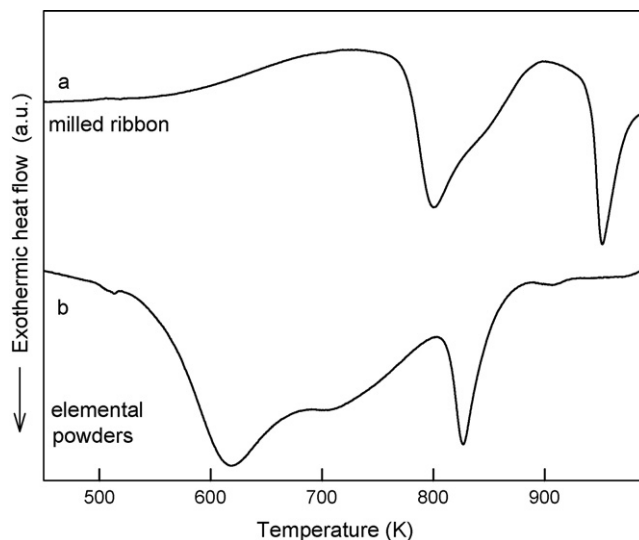


Fig. 3. DSC curves of the powders prepared by milling (a) the amorphous ribbon and (b) the elemental powders.

ues of the hyperfine field related to the amorphous phase are 24.0 and 23.7 T for the as-quenched and as-milled samples, respectively.

The DSC curve obtained for the as-milled sample exhibits three exothermic peaks (Fig. 3a). In order to study phase transformations induced by thermal treatment the powder samples were heated up to the characteristic temperatures determined from the DSC curve. The heating of the powder up to 798 K (temperature of the first peak) caused partial crystallization of the bcc FeCo phase with average grain size of 8 nm as revealed by the appearance of the bcc lines in the XRD pattern (Fig. 2). The Mössbauer spectrum recorded for this sample consists of two sextets: one with hyperfine field of 35.7 T, corresponding to the bcc FeCo phase, and the other one with broadened lines and average hyperfine field of about 23 T related to the remaining amorphous phase (Fig. 1c). The relative content of the FeCo subspectrum is 49%. The heating of the amorphous powder up to 893 K, that is higher than the temperature of the second poorly resolved exothermic peak, induced further crystallization of the FeCo phase (Fig. 2). The average grain size of this phase increased slightly to about 10 nm. The relative content of the FeCo phase determined from the Mössbauer spectrum is 68%. Beside the dominating FeCo sextet two new components appeared in the spectrum (Fig. 1d). The sextet with broad lines and a reduced hyperfine field of about 31 T can be assigned to disordered regions like grain boundaries. The relatively large spectral contribution of this component (22%) and nanometer size of the FeCo grains indicate the formation of the nanocrystalline structure. The quadrupole doublet with quadrupole splitting of 0.55 mm/s and isomer shift close to 0.00 mm/s is also observed in the Mössbauer spectrum (Fig. 1d). It originates most probably from the Fe atoms surrounded by Zr ones. The third exothermic peak on the DSC curve is related to the formation of iron borides. The XRD pattern obtained after the heating of the powder up to 993 K reveals mainly the lines corresponding to the bcc FeCo and  $(\text{Fe}, \text{Ni})_{23}\text{B}_6$ -type phases,

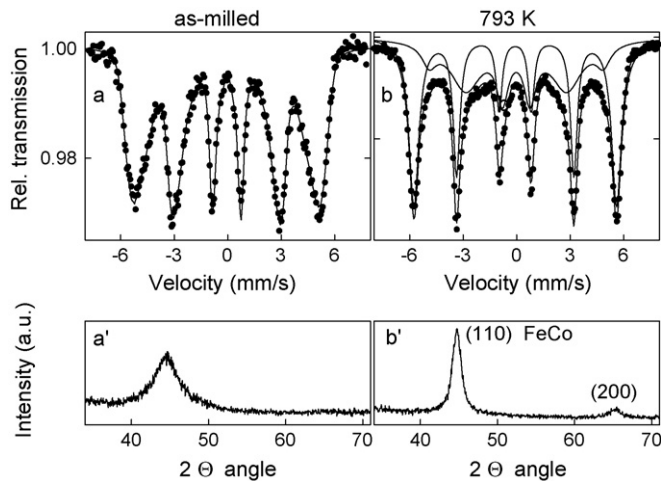


Fig. 4. Mössbauer spectra (a and b) and the corresponding XRD patterns (a' and b') of the as-milled and heated powders prepared by milling the elemental powders.

however, traces of other iron-based borides can be also present (Fig. 2).

The Mössbauer and XRD results of the samples prepared by mechanical alloying of the mixture of crystalline elemental powders with the composition of  $\text{Fe}_{41}\text{Ni}_{20}\text{Co}_{20}\text{Zr}_7\text{B}_{12}$  for 200 h are shown in Fig. 4. The XRD pattern of the as-milled sample (Fig. 4a') resembles the one obtained for the amorphous powder prepared from the ribbon (Fig. 2). However, the Mössbauer spectrum consists of the broadened sextet with hyperfine field of 28.9 T (Fig. 4a), that is markedly larger than that observed for the amorphous ribbon and powder, suggesting the crystalline structure of the mechanically alloyed sample. The results indicate that ball milling of the elemental powders did not induce an amorphization process but led to the formation of the nanocrystalline iron-based random solid solution. As it was shown in [2] a possible reason for the formation of the non-amorphous structure in FeCoNiZrB alloys by mechanical alloying could be a relatively large amount of Co atoms that would prevent the diffusion of other alloying elements into the bcc Fe and hence prevent the solid-state amorphization. Among the Fe–X pairs (X, alloying element) the Fe–Co one has the smallest negative value of the heat of mixing. Another reason for the formation of the nanocrystalline solid solution by mechanical alloying are small differences in the atomic sizes of Fe, Co and Ni that do not limit significantly the solubilities of these elements in their crystalline phases.

Thermal behaviour of the mechanically alloyed sample studied by DSC is similar to the case of the as-milled ribbon, however, crystallization temperatures determined for the nanocrystalline powder are much lower than those obtained for the amorphous one (Fig. 3). Heating of the nanocrystalline powder up to 793 K caused the formation of the bcc FeCo phase as shown in Fig. 4b and b'. The appearance of the sextet with hyperfine field of 35.3 T, characteristic for the bcc FeCo phase, is clearly observed in the Mössbauer spectrum. The estimated average grain size and the relative content of this phase are 7 nm and 55%, respectively.

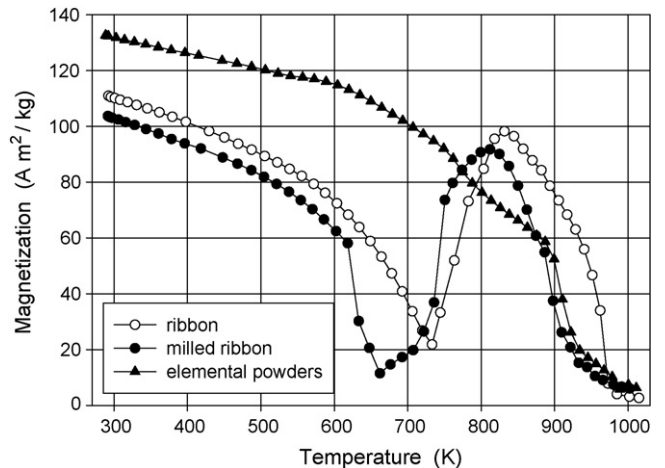


Fig. 5. Temperature variation of magnetization of the as-quenched ribbon and powders prepared by milling of the amorphous ribbon and elemental powders.

Temperature variation of magnetization is typical for the strong ferromagnetic ordering of the systems studied (Fig. 5). The room temperature values of magnetic moment per formula unit equal to 1.07 and  $1.01\mu_B$  for the as-quenched and ball milled ribbons, respectively. These values are somewhat lower as compared to  $1.28\mu_B$  for the mechanically alloyed mixture of crystalline elements. Such a ratio of the effective magnetic moments is due to the topological and chemical disorder in the amorphous phase. The Curie temperature of the amorphous phase is about 706 and 633 K for the as-quenched and milled ribbons, respectively. The characteristic increase in magnetization reveals that the crystallization starts around 735 and 665 K for the amorphous ribbon and powder, respectively, and corresponds to partial crystallization of the bcc FeCo. The temperature variation of magnetization shows that crystallization occurs in the relatively broad temperature intervals up to 830 and 810 K, respectively. This stage completes the crystallization of the bcc phase followed by the formation of iron borides. The Curie temperatures of the crystalline phases in the ribbon and milled ribbon samples are as high as 962 and 898 K, respectively. Magnetization of the powder prepared by mechanical alloying of crystalline elements for 200 h decreases monotonically as temperature increases, showing no distinct crystallization temperature as it was observed for the amorphous samples. The Curie temperature for this sample equals to 910 K, being very close to the one estimated for the crystallized ball milled ribbon. The magnetic measurements confirm the formation of the nanocrystalline iron-based solid solution due to the mechanical alloying of the elemental powders.

#### 4. Conclusions

The amorphous powder was prepared by ball milling of the  $\text{Fe}_{41}\text{Ni}_{20}\text{Co}_{20}\text{Zr}_7\text{B}_{12}$  amorphous ribbon. The mechanical alloying of the mixture of elemental powders led to the formation of

the nanocrystalline iron-based random solid solution as revealed by Mössbauer spectroscopy and magnetization measurements. The heat treatment of the as-milled amorphous and nanocrystalline powders caused at the first stage the crystallization of the bcc FeCo nanograins. Annealing at higher temperatures led to the formation of the bcc FeCo and iron-based boride phases. The Curie temperature of the amorphous phase estimated for the as-quenched ribbon is markedly higher than that of the amorphous powder.

## References

- [1] M. Kopcewicz, B. Idzikowski, J. Kalinowska, *J. Appl. Phys.* 94 (2003) 638–649.
- [2] Y.J. Liu, I.T.H. Chang, P. Bowen, *Mater. Sci. Eng. A* 304–306 (2001) 389–393.
- [3] A. Grabias, M. Kopcewicz, D. Oleszak, *J. Alloys Compd.* 339 (2002) 221–229.
- [4] A. Grabias, D. Oleszak, M. Kopcewicz, J. Latuch, T. Kulik, F. Stobiecki, *J. Non-Cryst. Solids* 330 (2003) 75–80.